Published OnlineFirst June 14, 2012; DOI: 10.1158/0008-5472.CAN-11-4092

Cancer Research

# PTEN and NF1 Inactivation in Schwann Cells Produces a Severe Phenotype in the Peripheral Nervous System That Promotes the Development and Malignant Progression of Peripheral Nerve Sheath Tumors

Vincent W. Keng, Eric P. Rahrmann, Adrienne L. Watson, et al.

*Cancer Res* 2012;72:3405-3413. Published OnlineFirst June 14, 2012.

Published OnlineFirst June 14, 2012; DOI: 10.1158/0008-5472.CAN-11-4092

*Tumor and Stem Cell Biology*

Cancer Research

# *PTEN* and *NF1* Inactivation in Schwann Cells Produces a Severe Phenotype in the Peripheral Nervous System That Promotes the Development and Malignant Progression of Peripheral Nerve Sheath Tumors

Vincent W. Keng[1,2,3,4], Eric P. Rahrmann[1,2,3,4], Adrienne L. Watson[1,2,3,4], Barbara R. Tschida[1,2,3,4], Christopher L. Moertel[4,5,6], Walter J. Jessen[7], Tilat A. Rizvi[7], Margaret H. Collins[8], Nancy Ratner[7], and David A. Largaespada[1,2,3,4,5]

## Abstract

The genetic evolution from a benign neurofibroma to a malignant sarcoma in patients with neurofibromatosis type 1 (NF1) syndrome remains unclear. Schwann cells and/or their precursor cells are believed to be the primary pathogenic cell in neurofibromas because they harbor biallelic *neurofibromin 1* (*NF1*) gene mutations. However, the *phosphatase and tensin homolog* (*Pten*) and neurofibromatosis 1 (*Nf1*) genes recently were found to be comutated in high-grade peripheral nerve sheath tumors (PNST) in mice. In this study, we created transgenic mice that lack both *Pten* and *Nf1* in Schwann cells and Schwann cell precursor cells to validate the role of these two genes in PNST formation *in vivo*. Haploinsufficiency or complete loss of *Pten* dramatically accelerated neurofibroma development and led to the development of higher grade PNSTs in the context of *Nf1* loss. *Pten* dosage, together with *Nf1* loss, was sufficient for the progression from low-grade to high-grade PNSTs. Genetic analysis of human malignant PNSTs (MPNST) also revealed downregulation of *PTEN* expression, suggesting that *Pten*-regulated pathways are major tumor-suppressive barriers to neurofibroma progression. Together, our findings establish a novel mouse model that can rapidly recapitulate the onset of human neurofibroma tumorigenesis and the progression to MPNSTs. *Cancer Res; 72(13); 3405–13. ©2012 AACR.*

## Introduction

Neurofibromatosis type 1 (NF1) syndrome is an autosomal dominant inherited disease in which a majority of patients develop benign plexiform and/or dermal neurofibromas. Of great concern is that approximately 10% of NF1 patients develop malignant peripheral nerve sheath tumors (MPNST), which often develop from plexiform neurofibromas and have a poor prognosis (1–3). Schwann cells are believed to be the primary pathogenic cell source in neurofibromas because they show biallelic *neurofibromin 1* (*NF1*) gene mutations (4–6). In addition to *NF1* mutations, MPNSTs harbor many secondary genetic changes and many of these underlying genetic mechanisms are still unknown (7).

Our laboratory and others have successfully shown the effectiveness of the conditional *Sleeping Beauty* (*SB*) transposon system as a forward genetic insertional mutagenesis screen in mice for cancer candidate genes (8–10). Using this *SB* system in a similar forward genetic screen to elucidate candidate genes responsible for sporadic MPNST formation, we directed *SB* insertional mutagenesis specifically in genetically predisposed Schwann cells and were successful in generating many tumors. We identified many candidate mutational drivers of higher grade peripheral nerve sheath tumors (PNST) by identifying commonly mutated genetic loci using the transposon as a molecular tag (manuscript in preparation). Importantly, *phosphatase and tensin homolog* (*Pten*) and *neurofibromatosis 1* (*Nf1*) genes were among the many candidate genes identified in this screen that tended to be comutated in the same high-grade PNSTs ($P < 7.94e{-}5$). Inactivation of the *Nf1* gene by the *desert hedgehog* (*Dhh*) promoter driving Cre recombinase (*Dhh*-Cre) at embryonic age 12.5 elicits plexiform neurofibromas, dermal neurofibromas, and abnormal hyperpigmentation (11). *PTEN*, a negative regulator of the *PI3K/AKT/mTOR* pathway involved in regulation of cell growth and survival, is the most frequently inactivated tumor suppressor gene in sporadic cancer (12). *Pten* dosage is essential for neurofibroma development and

**Authors' Affiliations:** [1]Masonic Cancer Center, [2]Department of Genetics, Cell Biology and Development, [3]Center for Genome Engineering, [4]Brain Tumor Program, Departments of [5]Pediatrics, [6]Pediatric Hematology and Oncology, University of Minnesota, Minneapolis, Minnesota; and Divisions of [7]Experimental Hematology and Cancer Biology, [8]Pathology and Laboratory Medicine, Cincinnati Children's Hospital Research Foundation, Cincinnati Children's Hospital Medical Center, Cincinnati, Ohio

**Note:** Supplementary data for this article are available at Cancer Research Online (http://cancerres.aacrjournals.org/).

Current address for W.J. Jessen: Biomarker Center of Excellence, Covance, Greenfield, IN.

**Corresponding Author:** David A. Largaespada, Masonic Cancer Center, Department of Genetics, Cell Biology and Development, Center for Genome Engineering, Brain Tumor Program, Department of Pediatrics, University of Minnesota, Minneapolis, MN 55455. Phone: 612-626-4979; Fax: 612-625-4648; E-mail: larga002@umn.edu

**doi:** 10.1158/0008-5472.CAN-11-4092

Published OnlineFirst June 14, 2012; DOI: 10.1158/0008-5472.CAN-11-4092



malignant transformation in the context of *Kras* activation (13). However, the relationship between *Pten* and *Nf1* in Schwann cell neurofibroma development and its progression to aggressive genetically engineered mouse model-PNST has not been elucidated. To further understand the underlying genetic complexity of plexiform neurofibroma and MPNST development, we hypothesized that somatic *Nf1* and *Pten* inactivation in Schwann cells and/or their precursors will promote progressive low-grade and/or high-grade PNST formation. *Dhh*-Cre was used to elicit recombination of $Nf1^{flox/flox}$ (14) and $Pten^{flox/flox}$ (15) alleles, allowing for inactivation of both *Nf1* and *Pten* genes in Schwann cells and/or their precursors. Knowing that *Dhh*-Cre; $Nf1^{flox/flox}$ (Δ*Nf1*) animals develop low-grade PNSTs, we hypothesized that triple transgenic mice *Dhh*-Cre; $Nf1^{flox/flox}$; $Pten^{flox/flox}$ (Δ*Nf1*/Δ*Pten*) could develop low-grade tumors that would further progress to high-grade PNSTs.

In this study, our data strongly implicates the synergistic role of *Pten* inactivation to plexiform neurofibroma tumorigenesis and progression to high-grade PNSTs in the context of *Nf1* loss in Schwann cells and/or their precursor cells. Importantly, expression microarray analyses of bulk tumor and cell lines from human NF1 patients also show a selective pressure towards loss of *PTEN* expression during disease progression from a benign neurofibroma to a malignant tumor. This novel mouse model can be used to rapidly model the onset of low-grade PNST development and its progression to high-grade PNSTs. In addition, this model can be used to test a variety of pharmaceutical agents *in vivo*.

## Materials and Methods

### Generation of transgenic animals

Generation of transgenic mice carrying the *Dhh* gene regulatory element driving Cre recombinase (*Dhh*-Cre) has been previously described (ref. 16; Supplementary Fig. S1). Transgenic mice carrying the floxed *Nf1* allele that has the essential exons 31 and 32 of the *Nf1* gene floxed with loxP sites has been previously described (ref. 14; Supplementary Fig. S1). The floxed *Pten* allele consists of the essential exons 4 and 5 of the *Pten* gene floxed with *lox*P sites has been previously described (ref. 15; Supplementary Fig. S1). These singly transgenic mice were crossed to obtain triple transgenic mice containing one allele of each transgene. These triple transgenic mice were then interbred to obtain various experimental and control cohorts (Fig. 1A). Animals were sacrificed when moribund because of paralysis and necropsy done. All animal work was conducted according to the University of Minnesota's approved animal welfare protocol.

### PCR genotyping

Identification of the various genotypes from both adult transgenic animal and pups were carried out as follows: Firstly, genomic DNA was isolated from tail clippings using standard proteinase K treatment, phenol–chloroform extraction and ethanol precipitation. Genomic DNA was then dissolved in sterile TE [10 mmol/L tris-HCl (pH7.5), 1 mmol/L EDTA (pH 8)] and quantified using a Nanodrop spectrophotometer. PCR genotyping was done using 50 ng of diluted genomic DNA as template in a 25 μL PCR reaction volume. PCR primers used for

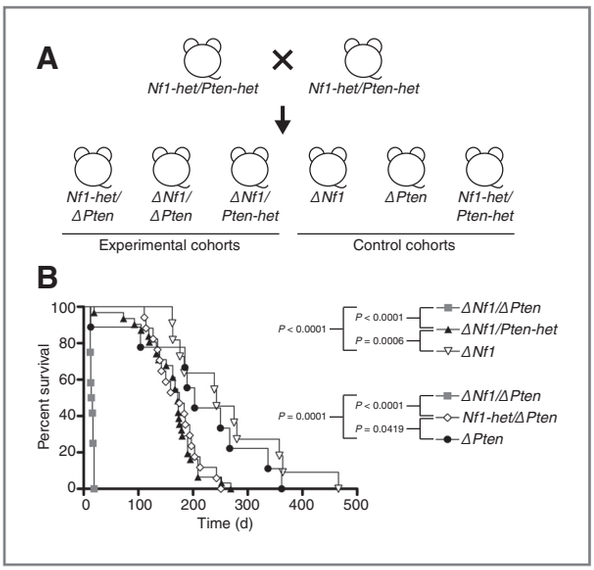


**Figure 1.** Establishing a novel peripheral nerve tumor progression mouse model. A, breeding strategy for generating experimental and control animals. Transgenic mice each carrying a single transgene was interbred to obtain doubly transgenic mice. Doubly transgenic mice were then interbred with remaining transgene to obtain triple transgenic *Dhh*-Cre; $Nf1^{flox/+}$; $Pten^{flox/+}$ mice (*Nf1-het/Pten-het*). Finally, triple transgenic mice were interbred to obtain the experimental and control cohorts required. *Dhh*-Cre; $Nf1^{flox/+}$; $Pten^{flox/flox}$ (*Nf1-het/*Δ*Pten*), *Dhh*-Cre; $Nf1^{flox/flox}$; $Pten^{flox/flox}$ (Δ*Nf1*/Δ*Pten*), and *Dhh*-Cre; $Nf1^{flox/flox}$; $Pten^{flox/+}$ (Δ*Nf1*/*Pten-het*) experimental cohorts. *Dhh*-Cre; $Nf1^{flox/flox}$ (Δ*Nf1*), *Dhh*-Cre; $Pten^{flox/flox}$ (Δ*Pten*) and *Nf1-het*/*Pten-het* control cohorts. B, Kaplan–Meier survival curves of various experimental and control cohorts generated using the GraphPad Prism software. *Pten* dosage augmented the peripheral nervous system phenotype in the context of *Nf1* inactivation in Schwann cell and/or their precursor cells. *P*, log-rank test.

*Dhh*-Cre were forward 5′-CTGGCCTGGTCTGGACACAGTGCCC-3′ and reverse 5′-CAGGGTCCGCTCGGGCATAC-3′ (amplicon 385 bp); *Nf1* floxed allele were wild type (WT) forward 5′-CTTCAGACTGATTGTTGTAACTGA-3′, WT reverse 5′-ACCTCTCTAGCCTCAGGAATGA-3′, and floxed reverse 5′-TGATTCCCACTTTGTGGTTCTAAG-3′ (WT amplicon 480 bp and floxed allele amplicon 350 bp); *Pten* floxed allele were forward 5′-AAAAGTTCCCCTGCTGATTTGT-3′ and reverse 5′-TGTTTTTGACCAATTAAAGTAGGCTGT-3′ (WT amplicon 310 bp and floxed allele amplicon 435 bp). PCR conditions for ReddyMix (Thermo Scientific) were used according to the manufacturer's instructions with an initial denaturing step of 95°C for 2 minutes; 30 or 35 cycles of denaturing at 95°C for 25 seconds, annealing at 55°C for 35 seconds and extension at 72°C for 65 seconds; followed by a final extension at 72°C for 5 minutes. PCR products were separated on a 2% agarose gel and genotype determined by the absence or presence of expected amplicons.

### Peripheral nerve tumor analysis

PNSTs were carefully removed from the sacrificed animal under a dissecting microscope (Leica), washed and placed in cold phosphate buffered saline (PBS). Any abnormal sciatic nerves, brachial plexi, and/or sacral plexi were also removed

Published OnlineFirst June 14, 2012; DOI: 10.1158/0008-5472.CAN-11-4092



when necessary. Trigeminal nerves attached to the brain were also observed for any abnormalities. The number of enlarged dorsal root ganglia was counted for the whole spinal cord. All reasonably sized tumor nodules (>1 mm in diameter) were carefully removed from the spinal cord using fine forceps and placed in fresh cold PBS.

### Hematoxylin and eosin staining

Sections for histology were only taken from larger tumor nodules (>1 mm in diameter). Tissues were fixed in 10% formalin, routinely processed and embedded in paraffin. Sections for histology were cut at 5 microns from the paraffin blocks using a standard microtome (Leica), mounted and heat fixed onto glass slides. Slides were either stained with hematoxylin and eosin (H&E) using standard protocols, or used for immunofluorescence, immunohistochemistry, and/or toluidine blue (TB) staining as described in the next section.

### Immunohistochemistry, toluidine blue, and immunofluorescence staining

Formalin-fixed paraffin-embedded sections from various tissues were sectioned at 5 microns, mounted and heat-fixed onto glass slides to be used for imunohistochemical analyses. Briefly, the glass section slides were dewaxed and rehydrated through a gradual decrease in ethanol concentration. The antigen epitopes on the tissue sections were then unmasked using a commercially available unmasking solution (Vector Laboratories) according to the manufacturer's instructions. The tissue section slides were then treated with 3% hydrogen peroxide to remove any endogenous peroxidases. Blocking was carried out at 4°C using a M.O.M. mouse immunoglobulin-blocking reagent (Vector Laboratories) or in appropriate normal serum from the host of the secondary antibody (5% serum in PBS) in a humidified chamber for several hours. For immunohistochemistry (IHC) and/or immunofluorescence, sections were then incubated overnight at 4°C in a humidified chamber using various primary antibodies at the indicated dilutions: Ki67 (1:200; Novocastra), S100β (1:100; Santa Cruz), Pten (1:200; Cell Signaling), phospho-Erk1/2 (1:400; Cell Signaling), phospho-Akt (Ser473; D9E; 1:250; Cell Signaling), Olig2 (1:200; Abcam) and phospho-S6 (Ser240/244; 1:200; Cell Signaling). After primary incubation, sections were washed thoroughly in PBS before incubating with horseradish peroxidase secondary antibody raised against the primary antibody initially used. After thorough washes with PBS, the sections were treated with freshly prepared DAB substrate (Vector Laboratories) and allowed for adequate signal to develop before stopping the reaction in water. Finally, sections were then lightly counterstained with hematoxylin, dehydrated through gradual increase in ethanol concentration, cleared in Citrosol, and mounted in Permount (Fisher).

TB staining for mast cells were carried out using standard protocols: Briefly, sections were dewaxed and rehydrated to water, stained with TB working solution (0.1% toluidine blue O in 0.9% sodium chloride pH 2.3) for 2 to 3 minutes, washed 3 times with distilled water before dehydrating quickly through a series of alcohols, clearing in Citrosol and finally mounted in Permount.

Immunofluorescence was carried out on formalin-fixed paraffin-embedded sections using standard techniques. Briefly, sections were processed as described previously for IHC up to the primary antibody incubation step. Sections were then incubated in fluorochrome-conjugated secondary antibodies (Invitrogen) before mounting in Prolong Gold Antifade Reagent (Invitrogen). Sections were examined using appropriate excitation wavelength.

### Histologic evaluation

Sections stained with H&E, antibodies to Ki67 and S100β antigens, and with TB were evaluated for all tumors (17). Each sample was graded using established criteria for tumors arising in genetically engineered mice (18, 19). Briefly, low-grade PNSTs exhibited low cellularity with little if any nuclear atypia and mitotic activity. High-grade PNSTs were increasingly cellular with increasing nuclear atypia and increasing mitotic activity.

### Microarray gene expression

Microarray gene expression analysis was done on purified human Schwann cells taken from normal sciatic nerve, dermal and plexiform neurofibromas, and MPNST cell lines as previously described (20, 21). Microarray gene expression analysis was also carried out on normal sciatic nerve tissue, dermal neurofibroma, plexiform neurofibroma, and malignant peripheral nerve sheath solid tumor samples obtained from NF1 patients as previously described (20, 21).

### Comparison of mouse model with human NF1 patients

MRI images of different neurofibromas were taken from NF1 patients at the University of Minnesota (IRB study number 1103E97613).

## Results

### Early postnatal lethality results from Nf1 and Pten inactivation in Schwann cells and/or their precursor cells

Transgenes used to generate the peripheral nerve tumor progression mouse model are shown in Supplementary Fig. S1. Transgenic mice carrying all 3 transgenes [*Dhh*-Cre; $Nf1^{flox/+}$; $Pten^{flox/+}$ (*Nf1-het*/*Pten-het*)] were interbred to generate both experimental and control cohorts (Fig. 1A). Significant differences in survival rate were observed between (i) *Dhh*-Cre; $Nf1^{flox/flox}$; $Pten^{flox/flox}$ (Δ*Nf1*/Δ*Pten*) and *Dhh*-Cre; $Nf1^{flox/flox}$; $Pten^{flox/+}$ (Δ*Nf1*/*Pten-het*; $P < 0.0001$, log-rank test) and (ii) Δ*Nf1*/*Pten-het* compared with *Dhh*-Cre; $Nf1^{flox/flox}$ (Δ*Nf1*; $P = 0.0006$, log-rank test), indicating *Pten* dosage in the context of *Nf1* inactivation plays an important role for disease progression (Fig. 1B).

In addition, significant differences in survival rate were also observed between (i) Δ*Nf1*/Δ*Pten* and *Dhh*-Cre; $Nf1^{flox/+}$; $Pten^{flox/flox}$ (*Nf1-het*/Δ*Pten*; $P < 0.0001$, log-rank test) and (ii) Δ*Nf1*/Δ*Pten* and *Dhh*-Cre; $Pten^{flox/flox}$ (Δ*Pten*; $P = 0.0001$, log-rank test; Fig. 1B). Complete inactivation of *Pten* in Schwann cells and/or their precursor cells alone can also contribute to enlarged dorsal root ganglia but at a lower penetrance (Supplementary Fig. S2). Although there was a statistical difference

Published OnlineFirst June 14, 2012; DOI: 10.1158/0008-5472.CAN-11-4092



**Table 1.** Occurrence of different peripheral nervous system phenotype in various experimental and control cohorts

| Genotype | *N* | Median survival age (d) | *n* | Enlarged DRG (mean ± SD) | Tumor grade | BP (%) | TN (%) | SN (%) | LP (%) |
|---|---|---|---|---|---|---|---|---|---|
| *Nf1*$^{f/f}$; *Pten*$^{f/f}$ | 12 | 15 | 11 | 21.8 ± 3.2 | High | 100 | 100 | 64 | 55 |
| *Nf1*$^{f/f}$; *Pten*$^{f/+}$ | 31 | 172 | 13 | 3.0 ± 1.8 | Low | 92 | 69 | 8 | 15 |
| *Nf1*$^{f/f}$ | 11 | 243 | 5 | 3.0 ± 1.0 | Low | 100 | 60 | 60 | 0 |
| *Nf1*$^{f/+}$; *Pten*$^{f/f}$ | 17 | 175 | 14 | 6.5 ± 4.0 | Low | 100 | 100 | 100 | 7 |
| *Pten*$^{f/f}$ | 9 | 203 | 7 | 7.1 ± 4.5 | Low | 100 | 86 | 71 | 14 |

NOTE: All mice were transgenic for *Dhh*-Cre. *f/f*, *flox/flox*; *f/+*, *flox/+*; *N*, total number of mice in each cohort; *n*, number of mice examined for the occurrence of various peripheral nervous system phenotype; DRG, number of enlarged dorsal root ganglia isolated (mean ± SD); grade, tumor grade was determined by histologic evaluation as described in the Materials and Methods. High, high-grade PNST; Low, low-grade PNST. Percentage of animals in each cohort that displayed the following peripheral nervous system phenotype: BP, enlarged brachial plexi; TN, enlarged trigeminal nerves; SN, enlarged sciatic nerves; LP, enlarged sacral plexi.

in the survival rate between Δ*Pten* and *Nf1-het*/Δ*Pten* cohorts ($P = 0.0419$, log-rank test), the occurrence of various peripheral nervous system phenotypes was comparable (Table 1). The median survival age for experimental and control cohorts are shown in Table 1. Experimental and control mice became moribund because of paralysis as the result of various peripheral nervous system tumor burden. In contrast, *Nf1-het*/*Pten-het* control mice ($n = 8$) displayed no obvious phenotype and were viable up to 365 days or more. Several *Nf1-het*/*Pten-het* control mice were sacrificed at various ages (from 189–506 days) and all peripheral nerves were normal (Supplementary Fig. S2).

There was also no statistically significant difference in survival rate between experimental cohorts Δ*Nf1*/*Pten-het* and *Nf1-het*/Δ*Pten* ($P = 0.7911$, log-rank test). Others and we have shown that Δ*Nf1* mice have a median survival age of about 243 days ($n = 11$) (11). There was no statistical difference in the survival rate between Δ*Pten* and Δ*Nf1* ($P = 0.3660$, log-rank test), indicating that loss of either tumor suppressor gene can promote Schwann cell tumorigenesis. Biallelic inactivation of *Nf1* and *Pten* in Schwann cells led to rapid postnatal death, resulting in a median survival age of 15 days (Fig. 1B). Increasing levels of *Pten* partially alleviated the severe phenotype, leading to an increase in survival (Fig. 1B). Complete *Nf1* loss is essential for the rapid severe peripheral nervous system phenotype in the context of *Pten* inactivation in Schwann cells and/or their precursor cells (Fig. 1B).

### Severe peripheral nervous system phenotype observed in Δ*Nf1*/Δ*Pten* animals

Δ*Nf1*/Δ*Pten* experimental animals displayed a severe early peripheral nervous system phenotype that included enlarged brachial plexi, multiple enlarged dorsal root ganglia, and enlarged trigeminal nerves (Fig. 2A, left). In contrast, Δ*Nf1*/*Pten-het* animals displayed a similar peripheral nervous system phenotype including enlarged brachial plexi, several large dorsal root ganglia, and enlarged trigeminal nerves but at a delayed latency (median age of 172 days) and at a significantly reduced tumor multiplicity (Fig. 2A, middle and Fig. 2B). Δ*Nf1* animals displayed a similar peripheral nervous system phenotype and at a similar tumor multiplicity but with a more delayed latency (median age of 243 days) compared with Δ*Nf1*/*Pten-het* animals (Fig. 2A, right). Both Δ*Nf1*/*Pten-het* and Δ*Nf1* animals had enlarged brachial plexi, several large dorsal root ganglia, and enlarged trigeminal nerves (Fig. 2A, middle and right, respectively). Importantly, *Pten* dosage with *Nf1* inactivation affected enlarged dorsal root ganglia tumor multiplicity between Δ*Nf1*/Δ*Pten* and Δ*Nf1*/*Pten-het* animals. Δ*Nf1*/Δ*Pten* animals had significantly more enlarged dorsal root ganglia, compared with Δ*Nf1*/*Pten-het* animals ($P < 0.0001$, unpaired *t* test; Fig. 2B and Table 1). *Pten* loss contributed to enlarged dorsal root ganglion formation as seen in *Nf1-het*/Δ*Pten* and Δ*Pten* animals. The median survival age and number of enlarged dorsal root ganglia from *Nf1-het*/Δ*Pten* and Δ*Pten* animals were shown in Supplementary Fig. S2 and Table 1. Both *Nf1-het*/Δ*Pten* and Δ*Pten* animals had an increased incidence of enlarged brachial plexi and trigeminal nerves (Supplementary Fig. S2 and Table 1). Enlarged peripheral nerves from *Nf1-het*/Δ*Pten* and Δ*Pten* animals were graded as low-grade PNSTs, whereas enlarged peripheral nerves from Δ*Nf1*/Δ*Pten* experimental animals were graded as high-grade PNSTs by histology and Ki67 staining criteria as depicted (refs. 18, 19; Table 1). Δ*Nf1*/Δ*Pten* experimental animals had enlarged brachial plexi and trigeminal nerves at 100% occurrence ($n = 11$), whereas Δ*Nf1*/*Pten-het* animals had enlarged brachial plexi and trigeminal nerves at 92.3% and 69.2% occurrence ($n = 13$), respectively (Table 1). Occurrence of other peripheral nerve phenotype seen in Δ*Nf1*/Δ*Pten* experimental animals ($n = 11$) included enlarged lumbar sacral plexi (54.5%) and enlarged sciatic nerves (63.6%; Table 1). It seems that *Pten* inactivation was required for lumbar plexi tumorigenesis, and that a dose-dependent effect exists as more tumors were found in animals with both alleles inactivated compared with animals with one allele inactivated. As for Δ*Nf1*/*Pten-het* animals ($n = 13$), occurrence of enlarged lumbar sacral plexi

Published OnlineFirst June 14, 2012; DOI: 10.1158/0008-5472.CAN-11-4092



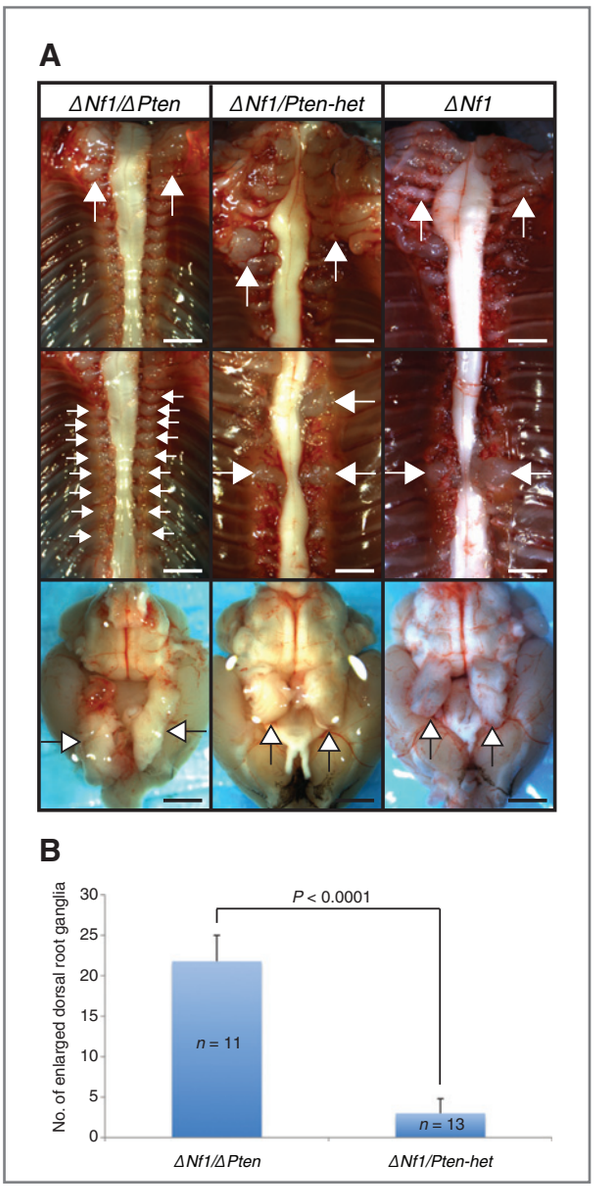


**Figure 2.** *Pten* dosage with *Nf1* inactivation affected enlarged dorsal root ganglia tumor multiplicity. A, left, representative of an early onset peripheral nervous system phenotype observed in a 16-day *Dhh*-Cre; $Nf1^{flox/flox}$; $Pten^{flox/flox}$ (*ΔNf1/ΔPten*) experimental mouse. Enlarged brachial plexus, majority of dorsal root ganglia enlarged, and enlarged trigeminal nerves. Middle, representative of a late onset peripheral nervous system phenotype observed in a 163 day *Dhh*-Cre; $Nf1^{flox/flox}$; $Pten^{flox/+}$ (*ΔNf1/Pten-het*) experimental mouse. Enlarged brachial plexus, several enlarged dorsal root ganglia, and enlarged trigeminal nerves. Right, representative of a late onset peripheral nervous system phenotype observed in a 184-day *Dhh*-Cre; $Nf1^{flox/flox}$ (*ΔNf1*) control mouse. Enlarged brachial plexus, several enlarged dorsal root ganglia, and enlarged trigeminal nerves. Top, brachial plexi; middle, dorsal root ganglia; bottom, brain with trigeminal nerves; arrows indicate peripheral nervous system phenotype; scale bars, 2 mm. B, statistically significant differences in the number of enlarged dorsal root ganglia isolated from each experimental cohort when animals became moribund (median survival ages for *ΔNf1/ΔPten* and *ΔNf1/Pten-het* were 15 and 163 days, respectively). Mean ± SD; *P*, unpaired *t* test; *n*, number of mice evaluated in each cohort.

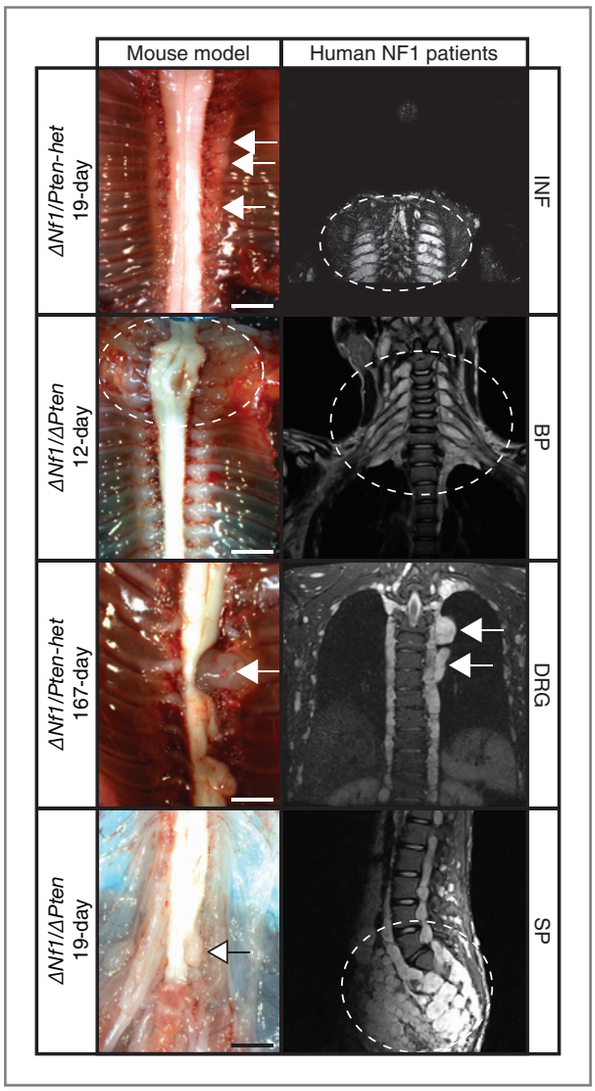


**Figure 3.** Recapitulating the human NF1 condition using mouse models. The various peripheral nervous system phenotype shown by *Dhh*-Cre; $Nf1^{flox/flox}$; $Pten^{flox/flox}$ (*ΔNf1/ΔPten*) and *Dhh*-Cre; $Nf1^{flox/flox}$; $Pten^{flox/+}$ (*ΔNf1/Pten-het*) experimental animals at various ages indicated (left) clearly recapitulates the human NF1 disease as depicted in the MRI images (right). INF, intercostal neurofibromas; BP, enlarged brachial plexi; DRG, enlarged dorsal root ganglia; SP, enlarged lumbar sacral plexi. Arrows and dashed lines indicate peripheral nervous system phenotype. Scale bars, 2 mm.

and sciatic nerves were seen at 15.4% and 7.7%, respectively (Table 1). The occurrence of various peripheral nerve phenotypes in other experimental and control cohorts is shown in Table 1.

### Mouse model recapitulates the human disease

Importantly, *ΔNf1/ΔPten* and *ΔNf1/Pten-het* experimental animals generated in this study showed various phenotypes that recapitulate the human NF1 disease (Fig. 3). These phenotypes included intercostal and paraspinal neurofibromas and enlarged brachial and lumbar sacral plexi.

Published OnlineFirst June 14, 2012; DOI: 10.1158/0008-5472.CAN-11-4092



### Histopathologic and immunohistochemical analyses revealed mice developed low-grade and high-grade PNSTs

Histopathologic and immunohistochemical analyses of peripheral nervous system tissues taken from both experimental cohorts showed high-grade PNSTs in Δ*Nf1*/Δ*Pten* animals (Fig. 4A) compared with low-grade PNSTs seen in Δ*Nf1*/*Pten-het* animals (Fig. 4B). Enlarged peripheral nervous system tissues taken from Δ*Pten* and *Nf1-het*/Δ*Pten* animals were generally low-grade PNSTs. Importantly, enlarged peripheral nerves taken from representative Δ*Nf1*/Δ*Pten* and Δ*Nf1*/*Pten-het* animals were positive for S100β and Olig2 staining, indicating a Schwann cell and/or precursor cell origin (Fig. 4A and B). These cells were also Ki67-positive at varying intensities indicative of cell proliferation (Fig. 4A and B). Enlarged peripheral nerves taken from Δ*Nf1*/Δ*Pten* and Δ*Nf1*/*Pten-het* animals were both pErk1/2 positive by IHC; levels were higher than detected in normal nerves (Supplementary Fig. S3), thus confirming that the conditional inactivation of *Nf1* in Schwann cells and/or their precursor cells resulted in activated *Ras*/*Mapk/Erk* signaling (Fig. 4A and B). Enlarged peripheral nerves taken from Δ*Nf1*/Δ*Pten* animals were also pAkt positive by IHC; levels were higher than detected in normal nerves (Supplementary Fig. S3), thus confirming the conditional inactivation of *Pten* in Schwann cells and/or their precursor cells results in activated *Pi3k*/*Akt*/*mTor* signaling (Fig. 4A). Similarly, *Nf1-het*/Δ*Pten* animals were also pAkt positive by IHC (Supplementary Fig. S3). In contrast, Δ*Nf1*/*Pten-het* animals were slightly positive for pAkt likely reflecting partial inactivation of *Pten* in Schwann cells and/or their precursor cells (Fig. 4B). Both Δ*Nf1*/Δ*Pten* and Δ*Nf1*/*Pten-het* animals were positive for pS6, a downstream effector gene and indicator for *Akt*/*mTor* activation (Fig. 4A and B). Interestingly, the wild-type Pten allele in Δ*Nf1*/*Pten-het* animals seemed to be intact, as peripheral nerves stained positive for Pten by immunofluorescence (Fig 4C). Semiquantitative analysis for Ki67-positive cells was carried out on representative peripheral nerves taken from control and experimental cohorts (Supplementary Fig. S4). There was no significant difference in number of Ki67-positive cells in cohorts with low-grade PNSTs (Table 1 and Supplementary Fig. S4). However, significant differences ($P < 0.01$) were seen in the number of Ki67-positive cells in Δ*Nf1*/Δ*Pten* animals with high-grade PNSTs when compared with other cohorts (Table 1 and Supplementary Fig. S4).

### Microarray gene expression analysis of human peripheral nerve tumor samples

Both *PTEN* and *NF1* levels in purified Schwann cells taken from human peripheral nerve, neurofibroma, and MPNST cell lines (Fig. 5A) and solid tumors (Fig. 5B) at various stages of disease were analyzed by microarray gene expression analysis. As expected in NF1 patients, *NF1* expression levels were reduced in the majority of samples tested (Fig. 5A and B). Although there may be a trend to reduced *PTEN* expression levels at early stages of the disease, there was a dramatic decrease in its expression level in the malignant stage of the disease (Fig. 5A and B).

## Discussion

This study shows that conditional inactivation of both *Nf1* and *Pten* genes in Schwann cells and/or their precursor cells results in lethality by 15 days after birth. Histopathologic analyses of enlarged peripheral nerves isolated from Δ*Nf1*/Δ*Pten* animals classified tumors as high-grade PNSTs, in contrast to the low-grade PNSTs in Δ*Nf1*/*Pten-het* animals. Interestingly, *Pten* dosage augmented the peripheral nervous system phenotype in the context of *Nf1* inactivation in Schwann cells and/or their precursor cells, but peripheral nervous system phenotype was not significantly affected by *Nf1* dosage in the context of *Pten* inactivation (Fig. 1B). It has also been previously shown that *Pten* dosage in mice is essential for neurofibroma development and malignant transformation, but not in the context of *Nf1* loss in Schwann cells and/or their precursor cells (13). Gregorian and colleagues used the *mGFAP*-Cre together with conditional *Nf1* and *Pten* alleles but found no tumors. This discrepancy in phenotype could be attributed to the different Cre used, which may represent a difference in the initiating cell type or strain background effects (13). Importantly, this conditional inactivation of *Pten* and *Nf1* mouse model can accurately recapitulate the different peripheral nervous phenotypes associated with the human NF1 syndrome (Fig. 3).

Human NF1 patients' neurofibromas seem to undergo changes that result in reduced *PTEN* expression during the progression from benign neurofibromas to MPNSTs (Fig. 5A and B). This may also be occurring in sporadic cases of MPNSTs as previous direct comparative microarray expression analyses showed no consistent differences between NF1-associated and sporadic MPNSTs (21). Thus, we propose that loss of *PTEN* is an important step in the malignant progression of neurofibromas. This hypothesis was further strengthened when in a separate forward genetic screen for genes responsible for sporadic MPNST using the *Sleeping Beauty* transposon insertional mutagenesis system, *Nf1* and *Pten* were identified as 2 potential mutational driver genes in the majority of high-grade PNSTs (manuscript in preparation).

Δ*Nf1*/*Pten-het* animals developed low-grade PNSTs earlier compared with Δ*Nf1* control animals, indicating that *Pten* dosage is important for neurofibroma tumorigenesis in the context of *Nf1* loss in Schwann cells and/or their precursor cells. There was no statistical difference in the survival rate between Δ*Pten* and Δ*Nf1* ($P = 0.3660$, log-rank test), indicating that loss of either tumor suppressor gene can promote Schwann cell tumorigenesis. Constitutive activation of either *Ras*/*Mapk/Erk* or *Pi3k*/*Akt*/*mTor* pathways alone may not be sufficient for tumor initiation and/or progression as Δ*Nf1* and Δ*Pten* animals control animals develop a peripheral nervous system phenotype similar to one another (Table 1). When one allele of *Pten* was inactivated in the context of *Nf1* loss to allow for partial activation of the *Pi3k*/*Akt*/*mTor* pathway, we observed a significantly reduced latency in tumorigenesis when compared with animals with *Nf1* inactivated only. As Δ*Nf1*/*Pten-het* tumors retained Pten protein expression (Fig. 4C), this result suggests that *Pten* is haploinsufficient for tumor suppression in this context. Genetic events that reduce *PTEN*

Published OnlineFirst June 14, 2012; DOI: 10.1158/0008-5472.CAN-11-4092



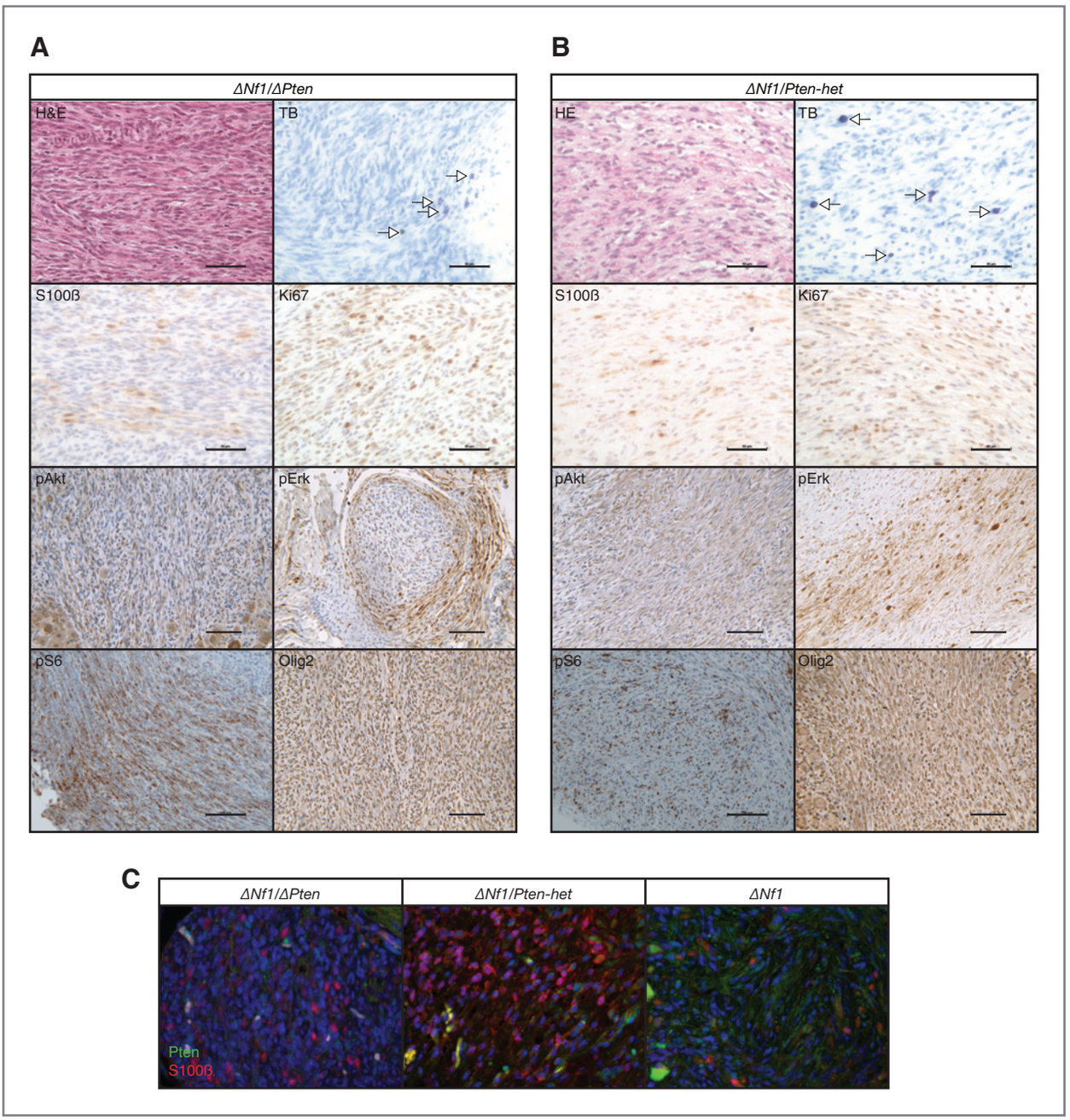


**Figure 4.** Histologic analyses of peripheral nervous system phenotype. Standard H&E and TB staining were carried out on all peripheral nervous system tissue sections (A and B). Immunohistochemical staining using antibodies against the proliferative marker (Ki67), Schwann cell/oligodendrocyte lineage marker (S100ß and Olig2), activated *Ras/Mapk/Erk* signaling by phospho-Erk1/2 (pErk), activated *Pi3k/Akt* signaling by phospho-Akt detection, and activated *mTor* signaling by phospho-S6 (pS6) [A and B]. Negative controls, sections incubated without the primary antibody gave no significant signal above background. A, representative H&E, TB, and immunohistochemical analyses of enlarged peripheral nerve from a representative *Dhh*-Cre; $Nf1^{floxflox}$; $Pten^{flox/flox}$ (*ΔNf1/ΔPten*) experimental mouse. Scale bars, 50 μm. B, representative H&E, TB, and immunohistochemical analyses of enlarged peripheral nerve from a representative *Dhh*-Cre; $Nf1^{floxflox}$; $Pten^{flox/+}$ (*ΔNf1/Pten-het*) experimental mouse. Scale bars, 50 μm. Representative immunohistochemical staining showing elevated pErk levels in peripheral nerves taken from *ΔNf1/ΔPten* and *ΔNf1/Pten-het* animals likely as a result of *Nf1* inactivation. Scale bar, 100 μm. Representative imunohistochemical staining showing elevated pAkt levels in peripheral nerve from a *ΔNf1/ΔPten* animal but only slightly elevated levels in a *ΔNf1/Pten-het* animal likely as a result of *Pten* gene dosage response. Scale bar, 100 μm. Representative imunohistochemical staining showing elevated pS6 levels in peripheral nerve from a *ΔNf1/ΔPten* animal but only slightly elevated levels in a *ΔNf1/Pten-het* animal. Scale bar, 100 μm. Arrows in TB-stained panels indicate mast cells (A and B). C, representative fluorescent images showing increase in Pten protein levels as gene dosage increases in *ΔNf1/ΔPten*, *ΔNf1/Pten-het*, and *Dhh*-Cre; $Nf1^{floxflox}$ (*ΔNf1*) animals. Peripheral nerves were costained with an anti-S100β (red channel) to identify Schwann cells, 4′, 6-diamidino-2-phenylindole (blue channel) to identify nuclei, and anti-Pten (green channel) to detect Pten protein status.

Published OnlineFirst June 14, 2012; DOI: 10.1158/0008-5472.CAN-11-4092



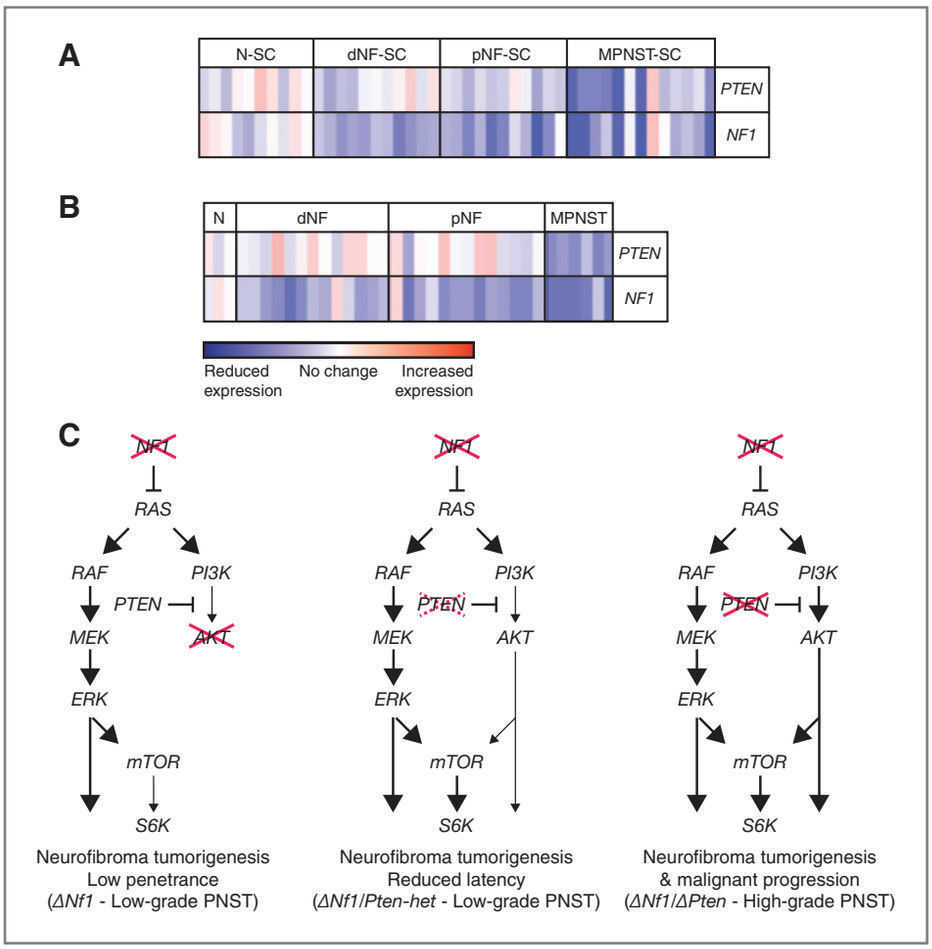


**Figure 5.** Expression microarray analysis of *PTEN* and *NF1* in human peripheral nerve tumors. A, purified human Schwann cells from normal sciatic nerve (N-SC), dermal neurofibroma cell lines (dNF-SC), plexiform neurofibroma cell lines (pNF-SC), and malignant peripheral nerve sheath cell lines (MPNST-SC). B, normal human sciatic nerve tissues (N) and solid tumors from dermal neurofibromas (dNF), plexiform neurofibromas (pNF), and malignant peripheral nerve sheath tumors (MPNST). As expected, there was a reduction in *NF1* expression levels from all stages of the disease. As the disease progressed from a benign to malignant form, decrease in *PTEN* expression was observed. Red, increase in red intensity as expression increases; blue, increase in blue intensity as expression decreases. C, conditional inactivation of *Nf1* in Schwann cells and/or their precursor cells resulted in low-grade PNST tumorigenesis at low penetrance (left). However, partial conditional inactivation of *Pten* in the context of *Nf1* loss in Schwann cells and/or their precursor cells resulted in reduced latency of low-grade PNST tumorigenesis when compared with mice with *Nf1* conditional inactivation only. Genetic events that reduce *PTEN* expression or activity are likely to be strongly selected for during MPNST progression (middle). In contrast, conditional inactivation of both *Pten* and *Nf1* in Schwann cells and/or their precursor cells resulted in high-grade PNST initiation and/or progression due to the upregulation of both *Ras/Mapk/Erk* and *Pi3k/Akt/mTor* signaling pathways (right). *Dhh*-Cre; $Nf1^{flox/flox}$ (Δ*Nf1*), *Dhh*-Cre; $Nf1^{flox/flox}$; $Pten^{flox/+}$ (Δ*Nf1/Pten-het*) and *Dhh*-Cre; $Nf1^{flox/flox}$; $Pten^{flox/flox}$ (Δ*Nf1/*Δ*Pten*) animals.

expression or activity are likely to be strongly selected for during MPNST progression. Thus, therapeutic agents that target *PI3K/AKT* signaling may be very useful for MPNST treatment or prevention strategies. Latency was further reduced and transformation augmented when both *Nf1* and *Pten* were inactivated, increasing tumor multiplicity and disease progression from low-grade to high-grade PNSTs, with both *Ras/Mapk/Erk* and *Pi3k/Akt/mTor* pathways activated (Fig. 4A and 5C). It has been shown that the activation of the *PI3K/AKT* and *MAPK/ERK* signaling pathways may be responsible for the underlying biologic aggressiveness in human pilocytic astrocytomas, a condition also found in NF1 patients (22). This could be precisely what is occurring in this novel mouse model with conditional inactivation of *Nf1* and *Pten* in Schwann cells, as evident with the rapid manifestation of high-grade PNSTs. Staining for pS6 in both Δ*Nf1/*Δ*Pten* and Δ*Nf1/Pten-het* peripheral nerves suggest activation of *mTor* signaling (Fig. 4A). However, hyperactivation of *mTor* signaling has also been shown in $Nf1^{-/-}$ astrocytes (23).

Taken together, these results suggest that *Pten* dosage, in the context of *Nf1* loss in Schwann cells and/or their precursor cells, is essential for the progression from low-grade to high-grade PNSTs. Interestingly, both Δ*Nf1/Pten-het* and Δ*Nf1/*Δ*Pten* animals generated a variety of different peripheral nervous system phenotype commonly seen in human NF1 patients, with higher penetrance and phenotypic diversity seen

Published OnlineFirst June 14, 2012; DOI: 10.1158/0008-5472.CAN-11-4092



in Δ*Nf1*/Δ*Pten* animals (Table 1). Thus, this model can be used to accurately recapitulate the human disease and to potentially rapidly test a variety of pharmaceutical compounds *in vivo*.

## Disclosure of Potential Conflicts of Interest

D.A. Largaespada has ownership interest (including patents) in Discovery Genomics, Inc. He is also a consultant/Advisory Board member of Discovery Genomics, Inc.

## Authors' Contributions

**Conception and design:** V.W. Keng, E.P. Rahrmann, M.H. Collins, D.A. Largaespada
**Development of methodology:** V.W. Keng, E.P. Rahrmann, M.H. Collins
**Acquisition of data (provided animals, acquired and managed patients, provided facilities, etc.):** V.W. Keng, A.L. Watson, B.R. Tschida, C.L. Moertel, M. H. Collins, N. Ratner
**Analysis and interpretation of data (e.g., statistical analysis, biostatistics, computational analysis):** V.W. Keng, E.P. Rahrmann, A.L. Watson, C.L. Moertel, W.J. Jessen, M.H. Collins, N. Ratner
**Writing, review, and/or revision of the manuscript:** V.W. Keng, E.P. Rahrmann, A.L. Watson, C.L. Moertel, W.J. Jessen, M.H. Collins, N. Ratner
**Administrative, technical, or material support (i.e., reporting or organizing data, constructing databases):** V.W. Keng, B.R. Tschida
**Study supervision:** V.W. Keng
**Immunohistochemistry and histology:** T.A. Rizvi

## Grant Support

The work received funding from the NIH-NINDS-P50 N5057531 and the Margaret Harvey Schering Trust.

The costs of publication of this article were defrayed in part by the payment of page charges. This article must therefore be hereby marked *advertisement* in accordance with 18 U.S.C. Section 1734 solely to indicate this fact.

Received December 19, 2011; revised April 12, 2012; accepted April 16, 2012; published OnlineFirst June 14, 2012.

## References

1. Boyd KP, Korf BR, Theos A. Neurofibromatosis type 1. J Am Acad Dermatol 2009;61:1–14; quiz 5–6.
2. Friedman JM. Epidemiology of neurofibromatosis type 1. Am J Med Genet 1999;89:1–6.
3. Rosenfeld A, Listernick R, Charrow J, Goldman S. Neurofibromatosis type 1 and high-grade tumors of the central nervous system. Childs Nerv Syst 2010;26:663–7.
4. Maertens O, Brems H, Vandesompele J, De Raedt T, Heyns I, Rosenbaum T, et al. Comprehensive NF1 screening on cultured Schwann cells from neurofibromas. Hum Mutat 2006;27:1030–40.
5. Serra E, Ars E, Ravella A, Sanchez A, Puig S, Rosenbaum T, et al. Somatic NF1 mutational spectrum in benign neurofibromas: mRNA splice defects are common among point mutations. Hum Genet 2001;108:416–29.
6. Serra E, Puig S, Otero D, Gaona A, Kruyer H, Ars E, et al. Confirmation of a double-hit model for the NF1 gene in benign neurofibromas. Am J Hum Genet 1997;61:512–9.
7. Carroll SL, Ratner N. How does the Schwann cell lineage form tumors in NF1? Glia 2008;56:1590–605.
8. Keng VW, Villanueva A, Chiang DY, Dupuy AJ, Ryan BJ, Matise I, et al. A conditional transposon-based insertional mutagenesis screen for genes associated with mouse hepatocellular carcinoma. Nat Biotechnol 2009;27:264–74.
9. Dupuy AJ, Rogers LM, Kim J, Nannapaneni K, Starr TK, Liu P, et al. A modified sleeping beauty transposon system that can be used to model a wide variety of human cancers in mice. Cancer Res 2009;69:8150–6.
10. Starr TK, Allaei R, Silverstein KA, Staggs RA, Sarver AL, Bergemann TL, et al. A transposon-based genetic screen in mice identifies genes altered in colorectal cancer. Science 2009;323:1747–50.
11. Wu J, Williams JP, Rizvi TA, Kordich JJ, Witte D, Meijer D, et al. Plexiform and dermal neurofibromas and pigmentation are caused by Nf1 loss in desert hedgehog-expressing cells. Cancer Cell 2008;13:105–16.
12. Hollander MC, Blumenthal GM, Dennis PA. PTEN loss in the continuum of common cancers, rare syndromes and mouse models. Nat Rev Cancer 2011;11:289–301.
13. Gregorian C, Nakashima J, Dry SM, Nghiemphu PL, Smith KB, Ao Y, et al. PTEN dosage is essential for neurofibroma development and malignant transformation. Proc Natl Acad Sci U S A 2009;106:19479–84.
14. Zhu Y, Ghosh P, Charnay P, Burns DK, Parada LF. Neurofibromas in NF1: Schwann cell origin and role of tumor environment. Science 2002;296:920–2.
15. Xiao A, Yin C, Yang C, Di Cristofano A, Pandolfi PP, Van Dyke T. Somatic induction of Pten loss in a preclinical astrocytoma model reveals major roles in disease progression and avenues for target discovery and validation. Cancer Res 2005;65:5172–80.
16. Jaegle M, Ghazvini M, Mandemakers W, Piirsoo M, Driegen S, Levavasseur F, et al. The POU proteins Brn-2 and Oct-6 share important functions in Schwann cell development. Genes Dev 2003;17:1380–91.
17. Viskochil DH. It takes two to tango: mast cell and Schwann cell interactions in neurofibromas. J Clin Invest 2003;112:1791–3.
18. Stemmer-Rachamimov AO, Louis DN, Nielsen GP, Antonescu CR, Borowsky AD, Bronson RT, et al. Comparative pathology of nerve sheath tumors in mouse models and humans. Cancer Res 2004;64:3718–24.
19. Weiss WA, Israel M, Cobbs C, Holland E, James CD, Louis DN, et al. Neuropathology of genetically engineered mice: consensus report and recommendations from an international forum. Oncogene 2002;21:7453–63.
20. Hummel TR, Jessen WJ, Miller SJ, Kluwe L, Mautner VF, Wallace MR, et al. Gene expression analysis identifies potential biomarkers of neurofibromatosis type 1 including adrenomedullin. Clin Cancer Res 2010;16:5048–57.
21. Miller SJ, Rangwala F, Williams J, Ackerman P, Kong S, Jegga AG, et al. Large-scale molecular comparison of human Schwann cells to malignant peripheral nerve sheath tumor cell lines and tissues. Cancer Res 2006;66:2584–91.
22. Rodriguez EF, Scheithauer BW, Giannini C, Rynearson A, Cen L, Hoesley B, et al. PI3K/AKT pathway alterations are associated with clinically aggressive and histologically anaplastic subsets of pilocytic astrocytoma. Acta Neuropathol 2011;121:407–20.
23. Dasgupta B, Yi Y, Chen DY, Weber JD, Gutmann DH. Proteomic analysis reveals hyperactivation of the mammalian target of rapamycin pathway in neurofibromatosis 1-associated human and mouse brain tumors. Cancer Res 2005;65:2755–60.